arXiv:hep-ex/0109018v2 24 Oct 2002

Searches for excited fermions in *ep* collisions at HERA

ZEUS Collaboration

Abstract

Searches in ep collisions for heavy excited fermions have been performed with the ZEUS detector at HERA. Excited states of electrons and quarks have been searched for in e^+p collisions at a centre-of-mass energy of $300\,\mathrm{GeV}$ using an integrated luminosity of $47.7\,\mathrm{pb}^{-1}$. Excited electrons have been sought via the decays $e^* \to e\gamma$, $e^* \to eZ$ and $e^* \to \nu W$. Excited quarks have been sought via the decays $q^* \to q\gamma$ and $q^* \to qW$. A search for excited neutrinos decaying via $\nu^* \to \nu\gamma$, $\nu^* \to \nu Z$ and $\nu^* \to eW$ is presented using e^-p collisions at $318\,\mathrm{GeV}$ centre-of-mass energy, corresponding to an integrated luminosity of $16.7\,\mathrm{pb}^{-1}$. No evidence for any excited fermion is found, and limits on the characteristic couplings are derived for masses $\lesssim 250\,\mathrm{GeV}$.

The ZEUS Collaboration

S. Chekanov, M. Derrick, D. Krakauer, S. Magill, B. Musgrave, A. Pellegrino, J. Repond, R. Yoshida
Argonne National Laboratory, Argonne, Illinois 60439-4815 [n]

M.C.K. Mattingly
Andrews University, Berrien Springs, Michigan 49104-0380

P. Antonioli, G. Bari, M. Basile, L. Bellagamba, D. Boscherini[1], A. Bruni, G. Bruni, G. Cara Romeo, L. Cifarelli[2], F. Cindolo, A. Contin, M. Corradi, S. De Pasquale, P. Giusti, G. Iacobucci, G. Levi, A. Margotti, T. Massam, R. Nania, F. Palmonari, A. Pesci, G. Sartorelli, A. Zichichi
University and INFN Bologna, Bologna, Italy [e]

G. Aghuzumtsyan, I. Brock, S. Goers, H. Hartmann, E. Hilger, P. Irrgang, H.-P. Jakob, A. Kappes[3], U.F. Katz[4], R. Kerger, O. Kind, E. Paul, J. Rautenberg, H. Schnurbusch, A. Stifutkin, J. Tandler, K.C. Voss, A. Weber, H. Wieber
Physikalisches Institut der Universität Bonn, Bonn, Germany [b]

D.S. Bailey[5], N.H. Brook[5], J.E. Cole, B. Foster, G.P. Heath, H.F. Heath, S. Robins, E. Rodrigues[6], J. Scott, R.J. Tapper, M. Wing
H.H. Wills Physics Laboratory, University of Bristol, Bristol, United Kingdom [m]

M. Capua, A. Mastroberardino, M. Schioppa, G. Susinno
Calabria University, Physics Department and INFN, Cosenza, Italy [e]

H.Y. Jeoung, J.Y. Kim, J.H. Lee, I.T. Lim, K.J. Ma, M.Y. Pac[7]
Chonnam National University, Kwangju, Korea [g]

A. Caldwell, M. Helbich, X. Liu, B. Mellado, S. Paganis, W.B. Schmidke, F. Sciulli
Nevis Laboratories, Columbia University, Irvington on Hudson, New York 10027 [o]

J. Chwastowski, A. Eskreys, J. Figiel, K. Klimek[8], K. Olkiewicz, M.B. Przybycień[9], P. Stopa, L. Zawiejski
Institute of Nuclear Physics, Cracow, Poland [i]

B. Bednarek, I. Grabowska-Bold, K. Jeleń, D. Kisielewska, A.M. Kowal[10], M. Kowal, T. Kowalski, B. Mindur, M. Przybycień, E. Rulikowska-Zarębska, L. Suszycki, D. Szuba, J. Szuba
Faculty of Physics and Nuclear Techniques, University of Mining and Metallurgy, Cracow, Poland [i]

A. Kotański
Department of Physics, Jagellonian University, Cracow, Poland

L.A.T. Bauerdick[11], U. Behrens, K. Borras, V. Chiochia, J. Crittenden[12], D. Dannheim, K. Desler[13], G. Drews, A. Fox-Murphy, U. Fricke, A. Geiser, F. Goebel, P. Göttlicher, R. Graciani, T. Haas, W. Hain, G.F. Hartner, K. Hebbel[14], S. Hillert, U. Kötz, H. Kowalski, H. Labes, B. Löhr, R. Mankel, J. Martens[15], M. Martínez[11], M. Milite, M. Moritz, D. Notz, M.C. Petrucci, A. Polini, U. Schneekloth, F. Selonke, S. Stonjek, B. Surrow[16], J.J. Whitmore[17], R. Wichmann[18], G. Wolf, C. Youngman, W. Zeuner
Deutsches Elektronen-Synchrotron DESY, Hamburg, Germany

C. Coldewey, A. Lopez-Duran Viani, A. Meyer, S. Schlenstedt
DESY Zeuthen, Zeuthen, Germany

G. Barbagli, E. Gallo, P. G. Pelfer
University and INFN, Florence, Italy [e]

A. Bamberger, A. Benen, N. Coppola, P. Markun, H. Raach[19], S. Wölfle
Fakultät für Physik der Universität Freiburg i.Br., Freiburg i.Br., Germany [b]

M. Bell, P.J. Bussey, A.T. Doyle, C. Glasman, S.W. Lee[20], A. Lupi, G.J. McCance, D.H. Saxon, I.O. Skillicorn
Department of Physics and Astronomy, University of Glasgow, Glasgow, United Kingdom [m]

B. Bodmann, N. Gendner, U. Holm, H. Salehi, K. Wick, A. Yildirim, A. Ziegler
Hamburg University, I. Institute of Exp. Physics, Hamburg, Germany [b]

T. Carli, A. Garfagnini, I. Gialas[21], E. Lohrmann
Hamburg University, II. Institute of Exp. Physics, Hamburg, Germany [b]

C. Foudas, R. Gonçalo[6], K.R. Long, F. Metlica, D.B. Miller, A.D. Tapper, R. Walker
Imperial College London, High Energy Nuclear Physics Group, London, United Kingdom [m]

P. Cloth, D. Filges
Forschungszentrum Jülich, Institut für Kernphysik, Jülich, Germany

M. Kuze, K. Nagano, K. Tokushuku[22], S. Yamada, Y. Yamazaki
Institute of Particle and Nuclear Studies, KEK, Tsukuba, Japan [f]

A.N. Barakbaev, E.G. Boos, N.S. Pokrovskiy, B.O. Zhautykov
Institute of Physics and Technology of Ministry of Education and Science of Kazakhstan, Almaty, Kazakhstan

S.H. Ahn, S.B. Lee, S.K. Park
Korea University, Seoul, Korea [g]

H. Lim[20], D. Son
Kyungpook National University, Taegu, Korea [g]

F. Barreiro, G. García, O. González, L. Labarga, J. del Peso, I. Redondo[23], J. Terrón,
M. Vázquez

Depto de Física Teórica, Universidad Autónoma Madrid, Madrid, Spain [l]

M. Barbi, A. Bertolin, F. Corriveau, A. Ochs, S. Padhi, D.G. Stairs, M. St-Laurent

Department of Physics, McGill University, Montréal, Québec, Canada H3A 2T8 [a]

T. Tsurugai

Meiji Gakuin University, Faculty of General Education, Yokohama, Japan

A. Antonov, V. Bashkirov[24], P. Danilov, B.A. Dolgoshein, D. Gladkov, V. Sosnovtsev,
S. Suchkov

Moscow Engineering Physics Institute, Moscow, Russia [j]

R.K. Dementiev, P.F. Ermolov, Yu.A. Golubkov, I.I. Katkov, L.A. Khein, N.A. Korotkova,
I.A. Korzhavina, V.A. Kuzmin, B.B. Levchenko, O.Yu. Lukina, A.S. Proskuryakov, L.M. Shche-
glova, A.N. Solomin, N.N. Vlasov, S.A. Zotkin

Moscow State University, Institute of Nuclear Physics, Moscow, Russia [k]

C. Bokel, J. Engelen, S. Grijpink, E. Koffeman, P. Kooijman, E. Maddox, S. Schagen,
E. Tassi, H. Tiecke, N. Tuning, J.J. Velthuis, L. Wiggers, E. de Wolf

NIKHEF and University of Amsterdam, Amsterdam, Netherlands [h]

N. Brümmer, B. Bylsma, L.S. Durkin, J. Gilmore, C.M. Ginsburg, C.L. Kim, T.Y. Ling

Physics Department, Ohio State University, Columbus, Ohio 43210 [n]

S. Boogert, A.M. Cooper-Sarkar, R.C.E. Devenish, J. Ferrando, J. Große-Knetter[14],
T. Matsushita, M. Rigby, O. Ruske[25], M.R. Sutton, R. Walczak

Department of Physics, University of Oxford, Oxford United Kingdom [m]

R. Brugnera, R. Carlin, F. Dal Corso, S. Dusini, S. Limentani, A. Longhin, A. Parenti,
M. Posocco, L. Stanco, M. Turcato

Dipartimento di Fisica dell' Università and INFN, Padova, Italy [e]

L. Adamczyk[26], L. Iannotti[26], B.Y. Oh, P.R.B. Saull[26], W.S. Toothacker[27]†
*Department of Physics, Pennsylvania State University, University Park, Pennsylvania
16802 [o]*

Y. Iga
Polytechnic University, Sagamihara, Japan [f]

G. D'Agostini, G. Marini, A. Nigro
Dipartimento di Fisica, Università 'La Sapienza' and INFN, Rome, Italy [e]

C. Cormack, J.C. Hart, N.A. McCubbin
Rutherford Appleton Laboratory, Chilton, Didcot, Oxon, United Kingdom [m]

C. Heusch
University of California, Santa Cruz, California 95064 [n]

I.H. Park
Seoul National University, Seoul, Korea

N. Pavel
Fachbereich Physik der Universität-Gesamthochschule Siegen, Germany

H. Abramowicz, S. Dagan, A. Gabareen, S. Kananov, A. Kreisel, A. Levy
Raymond and Beverly Sackler Faculty of Exact Sciences, School of Physics, Tel-Aviv University, Tel-Aviv, Israel [d]

T. Abe, T. Fusayasu, T. Kohno, K. Umemori, T. Yamashita
Department of Physics, University of Tokyo, Tokyo, Japan [f]

R. Hamatsu, T. Hirose, M. Inuzuka, S. Kitamura[28], K. Matsuzawa, T. Nishimura
Tokyo Metropolitan University, Deptartment of Physics, Tokyo, Japan [f]

M. Arneodo[29], N. Cartiglia, R. Cirio, M. Costa, M.I. Ferrero, S. Maselli, V. Monaco, C. Peroni, M. Ruspa, R. Sacchi, A. Solano, A. Staiano
Università di Torino, Dipartimento di Fisica Sperimentale and INFN, Torino, Italy [e]

D.C. Bailey, C.-P. Fagerstroem, R. Galea, T. Koop, G.M. Levman, J.F. Martin, A. Mirea, A. Sabetfakhri
Department of Physics, University of Toronto, Toronto, Ontario, Canada M5S 1A7 [a]

J.M. Butterworth, C. Gwenlan, R. Hall-Wilton, M.E. Hayes[14], E.A. Heaphy, T.W. Jones, J.B. Lane, M.S. Lightwood, B.J. West
Physics and Astronomy Department, University College London, London, United Kingdom [m]

J. Ciborowski[30], R. Ciesielski, G. Grzelak, R.J. Nowak, J.M. Pawlak, B. Smalska[31], T. Tymieniecka[32], A. Ukleja[32], J. Ukleja, J.A. Zakrzewski, A.F. Żarnecki
Warsaw University, Institute of Experimental Physics, Warsaw, Poland [i]

M. Adamus, P. Plucinski, J. Sztuk
Institute for Nuclear Studies, Warsaw, Poland [i]

Y. Eisenberg, L.K. Gladilin[33], D. Hochman, U. Karshon
Department of Particle Physics, Weizmann Institute, Rehovot, Israel [c]

J. Breitweg, D. Chapin, R. Cross, D. Kçira, S. Lammers, D.D. Reeder, A.A. Savin, W.H. Smith
Department of Physics, University of Wisconsin, Madison, Wisconsin 53706 [n]

A. Deshpande, S. Dhawan, V.W. Hughes P.B. Straub

Department of Physics, Yale University, New Haven, Connecticut 06520-8121 [n]

S. Bhadra, C.D. Catterall, W.R. Frisken, M. Khakzad, S. Menary

Department of Physics, York University, Ontario, Canada M3J 1P3 [a]

1 Introduction

The large number of quarks and leptons in the Standard Model suggests the possibility that they may be composite particles, consisting of combinations of more fundamental entities. The observation of excited states of quarks or leptons would be a clear signal that these particles are composite rather than elementary. At the electron[1]-proton collider HERA, excited electrons, quarks and neutrinos (e^*, q^*, ν^*) with masses up to the kinematic limit of $318\,\text{GeV}$ could be produced directly via t-channel exchange of a gauge boson as shown in Fig. 1: for e^*, via γ/Z exchange; for q^*, via $\gamma/Z/W$ exchange; and for ν^*, via W exchange. Once produced, the excited fermion (F^*) decays into a known fermion and a gauge boson.

This paper reports on searches for excited electrons and quarks in e^+p collisions and for excited neutrinos in e^-p collisions at HERA. From 1994 to 1997, the HERA collider operated with positron and proton energies of $27.5\,\text{GeV}$ and $820\,\text{GeV}$, respectively, resulting in a centre-of-mass energy of $300\,\text{GeV}$. A total of $47.7\,\text{pb}^{-1}$ of data were collected in the ZEUS detector during this period. This corresponds to a five-fold increase in statistics over the previously published ZEUS search with e^+p data [1]. A search for excited fermions based on $37\,\text{pb}^{-1}$ of e^+p data has been reported recently by the H1 collaboration [2]. In 1998 and 1999, the collider operated with e^- and with an increased proton energy of $920\,\text{GeV}$, resulting in a centre-of-mass energy of $318\,\text{GeV}$. The data collected with the ZEUS detector during this period correspond to an integrated luminosity of $16.7\,\text{pb}^{-1}$, leading to a 30-fold increase in statistics over the previous ZEUS publication with e^-p data [3].

2 Phenomenological model

It is convenient to choose a specific phenomenological model to quantify the experimental sensitivity which, for a narrow resonance, depends only on its mass and decay angular distribution. The most commonly used model [4,5,6] is based on the assumptions that the excited fermions have spin and isospin 1/2 and both left-handed, F_L^*, and right-handed components, F_R^*, are in weak isodoublets. The Lagrangian describes the transitions between known fermions, F_L, and excited states:

$$\mathcal{L}_{F^*F} = \frac{1}{\Lambda}\, \bar{F}_R^*\, \sigma^{\mu\nu} \left[g\, f\, \frac{\vec{\tau}}{2}\, \partial_\mu \vec{W}_\nu + g'\, f'\, \frac{Y}{2}\, \partial_\mu B_\nu + g_s\, f_s\, \frac{\lambda^a}{2}\, \partial_\mu G_\nu^a \right] F_L + \text{h.c.}\,, \qquad (1)$$

where Λ is the compositeness scale; $\vec{W}_\nu$, B_ν and G_ν^a are the $SU(2)$, $U(1)$ and $SU(3)$ fields; $\vec{\tau}$, Y and λ^a are the corresponding gauge-group generators; and g, g' and g_s are the

---

[1] Throughout this paper, "electron" is used generically to refer to e^+ as well as e^-.

coupling constants. The free parameters f, f' and f_s are weight factors associated with the three gauge groups and depend on the specific dynamics describing the compositeness. For an excited fermion to be observable, Λ must be finite and at least one of f, f' and f_s must be non-zero. By assuming relations between f, f' and f_s, the branching ratios of the excited-fermion decays can be fixed, and the cross section depends only on f/Λ.

For excited electrons, the conventional relation $f = f'$ is adopted. The dominant contribution to e^* production is t-channel γ exchange, in which roughly 50% of the excited electrons would be produced elastically [4].

For excited quarks, $f = f'$ is also adopted. There are stringent limits on f_s in q^* production from the Tevatron [7]. In this paper, f_s is set to zero, and the HERA sensitivity to the electroweak couplings f and f' is exploited. Under this assumption, q^* production via qg fusion vanishes and q^* does not decay into qg. Furthermore, a single mass-degenerate doublet (u^*, d^*) is assumed, so that the production cross-section arises from both u- and d-quark excitations.

Since excited-neutrino production requires W exchange, the cross section for $M_{\nu^*} > 200\,\mathrm{GeV}$ in e^-p collisions is two orders of magnitude higher than that in e^+p. Therefore, e^-p reactions offer much greater sensitivity for the ν^* search than e^+p reactions. In this paper, two very different assumptions are contrasted: the first uses $f = f'$, so that the photonic decay of the ν^* is forbidden; the second uses $f = -f'$, so that all ν^* decays into $\nu\gamma$, νZ and eW are allowed.

3   Experimental setup

A detailed description of the ZEUS detector can be found elsewhere [8]. A brief outline of the components that are most relevant for this analysis is given below.

Charged particles were tracked in the central tracking detector (CTD) [9], which operates in a magnetic field of $1.43\,\mathrm{T}$ provided by a thin superconducting coil. The CTD consists of 72 cylindrical drift-chamber layers, organized in 9 superlayers covering the polar-angle[2] region $15° < \theta < 164°$. The transverse-momentum resolution for full-length tracks is $\sigma(p_T)/p_T = 0.0058 p_T \oplus 0.0065 \oplus 0.0014/p_T$, with p_T in GeV.

The high-resolution uranium–scintillator calorimeter (CAL) [10] consists of three parts:

---

[2]   The ZEUS coordinate system is a right-handed Cartesian system, with the Z axis pointing in the proton beam direction, referred to as the "forward direction", and the X axis pointing left towards the centre of HERA. The coordinate origin is at the nominal interaction point. The pseudorapidity is defined as $\eta = -\ln\left(\tan\frac{\theta}{2}\right)$, where the polar angle, θ, is measured with respect to the proton beam direction. The azimuthal angle is denoted by ϕ.

the forward (FCAL), the barrel (BCAL) and the rear (RCAL) calorimeters. The calorimeters are subdivided transversely into towers, each of which subtends solid angles ranging from 0.006 to 0.04 steradians. Each tower is longitudinally segmented into one electromagnetic (EMC) section and either one (in RCAL) or two (in BCAL and FCAL) hadronic sections (HAC). Each HAC section consists of a single cell, while the EMC section of each tower is further subdivided transversely into four cells (two in RCAL). The CAL energy resolutions, as measured under test-beam conditions, are $\sigma(E)/E = 0.18/\sqrt{E}$ for electrons and $\sigma(E)/E = 0.35/\sqrt{E}$ for hadrons (E in GeV). The arrival time of CAL energy deposits is measured with sub-nanosecond resolution for energy deposits above 4.5 GeV, allowing the rejection of non-ep background.

The luminosity was measured using the Bethe-Heitler reaction $ep \rightarrow ep\gamma$ [11]. The resulting small-angle energetic photons were measured by the luminosity monitor, a lead-scintillator calorimeter placed in the HERA tunnel at $Z = -107\,\text{m}$.

A three-level trigger was used to select events online. The trigger criteria rely primarily on the energies deposited in the calorimeter. Timing cuts were used to reject beam-gas interactions and cosmic rays.

4   Monte Carlo simulation

The Monte Carlo (MC) event generator HEXF [12], based on the model of Hagiwara et al. [4], was used to simulate the excited-fermion signals. Initial-state radiation from the beam electron is included using the Weizsäcker-Williams approximation [13], and the hadronic final state is simulated using the matrix-element and parton-shower (MEPS) model of LEPTO 6.1 [14] for the QCD cascade and JETSET 7.4 [15] for the hadronisation.

The program DJANGO6 2.4 [16] was used to simulate backgrounds from neutral and charged current deep inelastic scattering (NC and CC DIS). The hadronic final state was simulated using the colour-dipole model as implemented in ARIADNE 4.08 [17] for the QCD cascade. The MEPS model was used to evaluate systematic uncertainties (see Section 7). Backgrounds from elastic and quasi-elastic QED-Compton scattering were simulated using COMPTON 2.0 [18]. Resolved and direct photoproduction (PHP) backgrounds were simulated with the HERWIG 5.9 [19] generator. PYTHIA 5.7 [20] was used to simulate backgrounds from the photoproduction of prompt photons. The EPVEC 1.0 [21] program was used to simulate W production.

All simulated events were passed through a detector simulation based on GEANT 3.13 [22] and were processed with the same reconstruction and analysis programs as used for the data.

5 Event selection

The selection used the following kinematic variables and particle-identification criteria:

- the scalar sum of the transverse energy deposited in the CAL, E_T;

- the vector sum of the transverse energy deposited in the CAL (missing transverse momentum), $\not{P}_t$;

- the difference between the total energy and the longitudinal momentum deposited in the CAL, $\delta = \sum_i E_i(1 - \cos\theta_i)$, where the energies of individual CAL cells are denoted by E_i and the angles θ_i are estimated from the geometric cell centres and the event vertex. For final states where no energy is lost through the rear beam-hole, the nominal value of δ should equal twice the electron-beam energy $(2E_e = 55\,\text{GeV})$;

- an identified electromagnetic (EM) cluster, which was required to have a minimum transverse energy (E_T^{EM}) of $10\,\text{GeV}$ and a polar angle of $\theta_{\text{EM}} < 2\,\text{rad}$. If the polar angle of the cluster was less than $0.3\,\text{rad}$, the threshold was raised to $E_T^{\text{EM}} > 30\,\text{GeV}$. An electromagnetic cluster was called "isolated" if the sum of the CAL energy not associated with this cluster but within an $\eta - \phi$ cone of radius 0.8 centered on the cluster was less than $2\,\text{GeV}$;

  - an EM cluster was identified as a photon candidate if no track measured by the CTD extrapolated to within 50 cm of the cluster;

  - an EM cluster was identified as an electron candidate if it had a track with a momentum greater than $5\,\text{GeV}$ that extrapolated to within 10 cm of the cluster. If its polar angle was less than $0.3\,\text{rad}$, the cluster was not required to have a matching track; such clusters may also be photon candidates;

- the following variables were calculated using CAL cells but excluding those with polar angles below $10°$, to avoid a contribution from the proton remnant:

  - the total invariant mass, M;

  - the hadronic invariant mass, M^{had}, and transverse energy, E_T^{had}, calculated excluding those CAL cells belonging to electron or photon candidates;

  - a second missing-transverse-momentum variable, $\not{P}_t(\theta > 10°)$.

To reduce the non-ep background, the reconstructed Z position of the interaction vertex was required to be within $\pm 50\,\text{cm}$ of the nominal interaction point. In addition, pattern-recognition algorithms were used to suppress non-ep backgrounds such as cosmic rays and beam-halo muons.

In the following, the selection criteria [1,3] used for the different decay modes are listed. These criteria were obtained from MC studies of signals and backgrounds with the goal of optimising sensitivities. Table 1 contains an overview of the decays.

5.1 Search for e^* production

The criteria used to select excited-electron candidates decaying into each of the four final states listed below are as follows:

a) $e^* \rightarrow e\gamma$:

- two isolated EM clusters, EM1 and EM2, each with $E_T^{\text{EM}} > 30\,\text{GeV}$;
- if both clusters are within the CTD acceptance, then one and only one of them was required to have a matching track;
- $35 < \delta < 65\,\text{GeV}$;
- $\theta_{\text{EM1}} + \theta_{\text{EM2}} < 2.5\,\text{rad}$.

b) $e^* \rightarrow \nu W \rightarrow \nu q'\bar{q}$:

- $P\!\!\!/_t > 25\,\text{GeV}$ and $P\!\!\!/_t(\theta > 10°) > 20\,\text{GeV}$;
- $10 < \delta < 50\,\text{GeV}$;
- either $E_T^{\text{had}} > 50\,\text{GeV}$ and $M^{\text{had}} > 60\,\text{GeV}$, or $E_T^{\text{had}} > 80\,\text{GeV}$ and $M^{\text{had}} > 40\,\text{GeV}$;
- events with an isolated electron were rejected.

c) $e^* \rightarrow eZ \rightarrow eq\bar{q}$:

- an electron[3] with $E_T^{\text{EM}} > 25\,\text{GeV}$;
- $35 < \delta < 65\,\text{GeV}$;
- either $E_T^{\text{had}} > 60\,\text{GeV}$ and $M^{\text{had}} > 80\,\text{GeV}$, or $E_T^{\text{had}} > 80\,\text{GeV}$ and $M^{\text{had}} > 40\,\text{GeV}$;
- $0.8 < M/M_{eZ} < 1.2$, where M_{eZ} is the electron-Z invariant mass defined in Section 6.

d) $e^* \rightarrow eZ \rightarrow e\nu\bar{\nu}$:

- an isolated electron;
- $P\!\!\!/_t > 20\,\text{GeV}$;
- $\cos(\phi_e - \phi_{\text{had}}) > -0.95$ if $E_T^{\text{had}} > 2\,\text{GeV}$, where ϕ_e and ϕ_{had} are the azimuthal angles of the electron and the hadronic system[4], respectively;
- $P\!\!\!/_t/E_T > 0.4$.

5.2 Search for q^* production

The following selection criteria were used for the excited-quark search:

a) $q^* \rightarrow q\gamma$:

---

[3] Since, in this channel, the electron can be close to a hadronic jet when the e^* mass is close to that of the Z, the electron was not required to be isolated.

[4] This cut rejects background from NC DIS events where the hadronic system balances the scattered electron back-to-back in ϕ.

- an isolated photon with $E_T^{\mathrm{EM}} > 20\,\mathrm{GeV}$ and $\theta_{\mathrm{EM}} < 1.2\,\mathrm{rad}$;
- $E_T^{\mathrm{had}} > 40\,\mathrm{GeV}$.

b) $q^* \rightarrow qW \rightarrow qe\nu$:

- an isolated electron with $E_T^{\mathrm{EM}} > 15\,\mathrm{GeV}$;
- $\displaystyle{\not}P_t > 18\,\mathrm{GeV}$;
- $\cos(\phi_e - \phi_{\mathrm{had}}) > -0.95$;
- $E_T^{\mathrm{had}} > 5\,\mathrm{GeV}$.

5.3 Search for ν^* production

The following cuts were applied to select excited neutrinos decaying into the three final states listed below:

a) $\nu^* \rightarrow \nu\gamma$:

- an isolated photon with $E_T^{\mathrm{EM}} > 20\,\mathrm{GeV}$;
- $\displaystyle{\not}P_t > 25\,\mathrm{GeV}$;
- $E_T > 50\,\mathrm{GeV}$;
- $\delta < 45\,\mathrm{GeV}$.

b) $\nu^* \rightarrow \nu Z \rightarrow \nu q\bar{q}$:

- the same cuts as used for $e^* \rightarrow \nu W \rightarrow \nu q'\bar{q}$ were applied.

c) $\nu^* \rightarrow eW \rightarrow eq'\bar{q}$:

- the same cuts as used for $e^* \rightarrow eZ \rightarrow eq\bar{q}$ were applied, except that the cut on M/M_{eZ} was replaced by the cut $0.9 < M/M_{eW} < 1.2$, where M_{eW} is the electron-W invariant mass defined in the next section.

6 Mass reconstruction of excited fermions

To improve the mass resolution, three kinematic constraints could be applied:

- the transverse momentum of the excited fermion was assumed to be zero. This was used except for $\nu^* \rightarrow \nu\gamma$;

- the longitudinal-momentum variable, δ, of the excited fermion's decay products was set to twice the electron-beam energy, the value expected when all decay products are observed. This assumption is less justified for decays of ν^* and q^* than for e^*, leading to worse resolutions for ν^* and q^*. Therefore, in the two cases $\nu^* \rightarrow \nu\gamma$ and $q^* \rightarrow q\gamma$, this constraint was not used;

- in all decays involving a final-state W or Z, the mass of their decay products was constrained to be the mass of the respective boson.

For $e^* \to e\gamma$, the electron-photon invariant mass was determined by the double-angle method [23] as

$$M_{e\gamma}^2 = (2E_e)^2 \left(\frac{\sin\theta_\gamma}{1 - \cos\theta_\gamma} \right) \left(\frac{\sin\theta_e}{1 - \cos\theta_e} \right) ,$$

where θ_e and θ_γ are the polar angles of the electron and photon, respectively.

For $q^* \to q\gamma$, the $q\gamma$ invariant mass was obtained from

$$M_{q\gamma}^2 = 2E_\gamma^2 \frac{\sin\theta_\gamma}{\sin\theta_{\text{had}}} \left[1 - \cos(\theta_\gamma + \theta_{\text{had}}) \right] ,$$

where E_γ and θ_{had} are the energy of the photon and the polar angle of the hadronic system, respectively.

For $\nu^* \to \nu\gamma$, the mass of the excited neutrino was determined from the invariant mass of the photon and the neutrino. The four-momentum of the neutrino was obtained using energy-momentum conservation.

For the excited-fermion decays to a fermion and a heavy vector boson, $F^* \to FV$, the mass was reconstructed using the energy and longitudinal momentum of the two decay products:

$$M_{FV}^2 = 2E_e(E^F + p_Z^F + E^V + p_Z^V) .$$

By using the relation

$$(E^V - p_Z^V)(E^V + p_Z^V) = M_V^2 + (E^F - p_Z^F)(E^F + p_Z^F) ,$$

the formula can be written as

$$M_{FV}^2 = 2E_e \frac{2E_e(E^F + p_Z^F) + M_V^2}{2E_e - (E^F - p_Z^F)} .$$

For $e^* \to eZ \to eq\bar{q}$, $e^* \to eZ \to e\nu\bar{\nu}$ and $\nu^* \to eW \to eq'\bar{q}$, the final-state electron energy and polar angle were used to obtain E^F and p_Z^F.

For $q^* \to qW \to qe\nu$, E^F and p_Z^F were obtained using the CAL cells with polar angle $\theta > 10°$, excluding those belonging to the electron.

For $e^* \to \nu W \to \nu q'\bar{q}$ and $\nu^* \to \nu Z \to \nu q\bar{q}$, the neutrino variables were obtained from the hadronic system using the relations $E^F - p_Z^F = 2E_e - \delta$ and $E^F + p_Z^F = \displaystyle{\not{P}}_t^2/(2E_e - \delta)$.

The Gaussian mass resolutions and the overall efficiencies after all selection cuts are listed in Table 2 for excited fermions with masses of 125 and 250 GeV.

7 Systematic uncertainties

The most important sources of systematic uncertainty were:

- the theoretical uncertainty on the production cross-section due to radiative corrections to the excited-fermion production model and to the uncertainties on the parton densities in the proton was taken to be 8%, as determined from an earlier study [3];

- the acceptance was determined using a simulation of spin-1/2 excited fermions. To estimate the effect of models assuming other spin states, the variation of the acceptance was evaluated by changing the nominal decay-angle distribution[5] to an isotropic one [3]. The variation was typically 5% or less;

- the energy scale of the calorimeter was varied by $\pm 3\%$, leading to uncertainties in the excited-fermion efficiency of at most 3%;

- the uncertainty on the measured integrated luminosity of the 1994–1997 $e^+ p$ data sample was 1.6% and that of the 1998–1999 $e^- p$ data sample was 1.8%.

8 Results

The number of observed events and the expected background for each channel are shown in Table 1. No significant excess of events is observed. The distributions of the invariant mass are compared[6] in Figs. 2 and 3 with the expected backgrounds for e^*, q^* and ν^*. No evidence for a resonance is seen.

Since there is no evidence for excited fermions, upper limits at 95% confidence level on f/Λ were derived. A Bayesian technique with the prior flat in $(f/\Lambda)^2$ was used. The limit on $\xi = f/\Lambda$ was given as the solution to $0.95 \int_0^\infty d\xi^2 \mathcal{L} = \int_0^{\xi_{\text{lim}}^2} d\xi^2 \mathcal{L}$ where

$$\mathcal{L}(\xi) = \int\limits_0^\infty d\gamma \frac{1}{\sqrt{2\pi}\sigma_\gamma} \exp \frac{-(\gamma-1)^2}{2\sigma_\gamma^2} \prod_c \left\{ p\left(N_c, \gamma(S_c(\xi) + B_c)\right) \prod_{i=1}^{N_c} \left(\frac{s_c(M_{ic}, \xi) + b_c(M_{ic})}{S_c(\xi) + B_c} \right) \right\}.$$

Here c labels the decay channel, N_c denotes the number of events observed in that channel and M_{ic} is the reconstructed mass of the i-th observed event. The probability to observe n events in a Poisson process with mean λ is denoted $p(n, \lambda)$. The expected reconstructed mass spectra for signal and background in channel c are denoted by s_c and b_c respectively. The number of expected signal events is given by $S_c(\xi) = \int dM s_c(M, \xi)$ and the expected

---

[5] For $F^* \to F\gamma$, for example, the nominal distribution is $(1 + \cos\theta^*)$, where θ^* is the polar angle between the incoming and outgoing fermions in the F^* rest frame.

[6] Only channels with more than ten candidate events are shown.

background is given by $B_c = \int dM b_c(M)$. Systematic uncertainties were taken into account by integration over γ, which has a Gaussian distribution with mean 1 and width $\sigma_\gamma = 0.123$. The systematic uncertainties degrade the limits by at most 4%.

The spectra of reconstructed mass, M, for the signals is calculated as

$$s_c(M, \xi) = L \int_0^\infty d\tilde{M} \sigma_{\mathrm{nwa}}(\tilde{M}, \xi) \frac{2\tilde{M} M_{F^*} \Gamma}{\left(\tilde{M}^2 - M_{F^*}^2\right)^2 + (M_{F^*}\Gamma)^2} \beta_c(\tilde{M}) \varepsilon_c(\tilde{M}) D_c(M, \tilde{M})$$

where L is the integrated luminosity, $\tilde{M}$ denotes the true mass of the produced excited fermion and M_{F^*} and Γ are the pole mass and the width. The total cross section in the narrow-width approximation is denoted σ_{nwa}. The functions $\beta_c(\tilde{M})$ and $\varepsilon_c(\tilde{M})$ respectively label the branching ratio and the detector acceptance for decay channel c. Detector resolution was described by the function $D_c(M, \tilde{M})$ which gives the probability density in M for events with true mass $\tilde{M}$, as obtained by a fit to simulated signal events. The function $D_c(M, \tilde{M})$ is a linear combination of a Gaussian in M with mean M_0 and a function of the form $[(\exp(\alpha(M - M_0)) + \exp(-\beta(M - M_0))]^{-1}$ with α and β positive. The latter function accounts for the tails of the mass spectrum.

Figure 4 shows limits on $\sigma \times BR$ under the assumption of a vanishing width. In this case $s_c(M, \xi)$ reduces to $L\sigma_{\mathrm{nwa}}(M_{F^*}, \xi)\beta_c(M_{F^*})\varepsilon_c(M_{F^*})D_c(M, M_{F^*})$. The limits were obtained using ARIADNE, the hadronisation model that gives the background estimate leading to the more conservative limits. The alternative choice of MEPS would have resulted in limits up to 12.5% more stringent.

Next, using the model [4,5,6] discussed in Section 2 to calculate the natural width Γ and the method described above, 95% confidence-level upper limits on f/Λ as a function of mass were calculated for excited electrons, quarks and neutrinos, shown in Fig. 5.

By assuming $f/\Lambda = 1/M_{F^*}$ and $f = f'$, excited fermions were excluded in the mass intervals from 100 up to 228 GeV for e^*, 205 GeV for q^*, and 135 GeV for ν^*. For $f = -f'$, excited neutrinos were excluded up to 158 GeV.

The exclusion limits on f/Λ are compared with corresponding direct limits from LEP experiments [24,25] in Fig. 5. The corresponding H1 limits on e^* and q^* [2] are comparable to those presented here. As seen in Fig. 5, the ZEUS limits extend to significantly higher masses than those of LEP. The present limits on f/Λ for q^* constrain the electroweak q^* couplings and are complementary to the limits on f_s set by CDF [7], which constrain the strong q^* coupling.

9 Conclusions

A search for heavy excited electrons which decay into $e\gamma$, eZ or νW has been performed using $47.7\,\text{pb}^{-1}$ of e^+p data at a centre-of-mass energy of $300\,\text{GeV}$ collected with the ZEUS detector at HERA during 1994 to 1997. There is no evidence for a narrow resonance decaying to any of the final states considered here. Upper limits at 95% confidence level on $\sigma \times BR$ and f/Λ have been derived. Assuming $f/\Lambda = 1/M_{e^*}$ and $f = f'$, excited electrons are excluded in the mass range $100\,\text{GeV}$ to $228\,\text{GeV}$.

The same data sample has been used to search for heavy excited quarks decaying to $q\gamma$ or qW. No evidence is found for such resonances, so that exclusion limits have been set. Assuming $f/\Lambda = 1/M_{q^*}$, $f = f'$ and $f_s = 0$, excited quarks are excluded in the mass range $100\,\text{GeV}$ to $205\,\text{GeV}$.

A search for heavy excited neutrinos which decay into $\nu\gamma$, νZ or eW has been performed using $16.7\,\text{pb}^{-1}$ of e^-p data at a centre-of-mass energy of $318\,\text{GeV}$ collected in 1998 and 1999. No resonance has been observed, and upper limits on $\sigma \times BR$ and f/Λ have been derived. Assuming $f/\Lambda = 1/M_{\nu^*}$ and $f = f'$ ($f = -f'$), excited neutrinos are excluded in the mass range $100\,\text{GeV}$ to $135\,(158)\,\text{GeV}$.

Acknowledgements

References

[1] ZEUS Collaboration, J. Breitweg et al., Z. Phys. C 76 (1997) 631.

[2] H1 Collaboration, C. Adloff et al., Eur. Phys. J. C 17 (2000) 567.

[3] ZEUS Collaboration, M. Derrick et al., Z. Phys. C 65 (1995) 627.

[4] K. Hagiwara, S. Komamiya and D. Zeppenfeld, Z. Phys. C 29 (1985) 115.

[5] U. Baur, M. Spira and P.M. Zerwas, Phys. Rev. D 42 (1990) 815.

[6] F. Boudjema, A. Djouadi and J.L. Kneur, Z. Phys. C 57 (1993) 425.

[7] CDF Collaboration, F. Abe et al., Phys. Rev. D 55 (1997) 5263.

[8] ZEUS Collaboration, U. Holm (ed.), *The ZEUS Detector*. Status Report (unpublished), DESY (1993), available on `http://www-zeus.desy.de/bluebook/bluebook.html`.

[9] N. Harnew et al., Nucl. Inst. Meth. A 279 (1989) 290;
B. Foster et al., Nucl. Phys. Proc. Suppl. B 32 (1993) 181;
B. Foster et al., Nucl. Inst. Meth. A 338 (1994) 254.

[10] M. Derrick et al., Nucl. Inst. Meth. A 309 (1991) 77;
A. Andresen et al., Nucl. Inst. Meth. A 309 (1991) 101;
A. Caldwell et al., Nucl. Inst. Meth. A 321 (1992) 356;
A. Bernstein et al., Nucl. Inst. Meth. A 336 (1993) 23.

[11] J. Andruszków et al., Preprint DESY-92-066, DESY, 1992;
ZEUS Collaboration, M. Derrick et al., Z. Phys. C 63 (1994) 391;
J. Andruszków et al., Acta Phys. Pol. B 32 (2001) 2025.

[12] H.J. Kim and S. Kartik, Preprint LSUHE-145-1993, 1993.

[13] Ch. Berger and W. Wagner, Phys. Rep. 146 (1987) 1.

[14] G. Ingelman, A. Edin and J. Rathsman, Comp. Phys. Comm. 101 (1997) 108.

[15] T. Sjöstrand, Comp. Phys. Comm. 39 (1986) 347;
T. Sjöstrand and M. Bengtsson, Comp. Phys. Comm. 43 (1987) 367;
T. Sjöstrand, Comp. Phys. Comm. 82 (1994) 74.

[16] K. Charchula, G.A. Schuler and H. Spiesberger, Comp. Phys. Comm. 81 (1994) 381;
H. Spiesberger, DJANGO6 *Version 2.4 – A Monte Carlo Generator for Deep Inelastic Lepton Proton Scattering Including QED and QCD Radiative Effects*, 1996, available on `http://www.desy.de/~hspiesb/django6.html`.

[17] L. Lönnblad, Comp. Phys. Comm. 71 (1992) 15.

[18] T. Carli et al., *Proc. Workshop on Physics at HERA*, W. Buchmüller and G. Ingelman (eds.), Vol. 3, p. 1468. Hamburg, Germany, DESY (1992).

[19] G. Marchesini et al., Comp. Phys. Comm. 67 (1992) 465.

[20] M. Bengtsson and T. Sjöstrand, Comp. Phys. Comm. 46 (1987) 43; T. Sjöstrand, *Pythia 5.6 and Jetset 7.3 Physics and Manual, CERN-TH.6488/92.* CERN, 1992.

[21] U. Baur, J.A.M. Vermaseren and D. Zeppenfeld, Nucl. Phys. B 375 (1992) 3.

[22] R. Brun et al., GEANT3, Technical Report CERN-DD/EE/84-1, CERN, 1987.

[23] S. Bentvelsen, J. Engelen and P. Kooijman, *Proc. Workshop on Physics at HERA*, W. Buchmüller and G. Ingelman (eds.), Vol. 1, p. 23. Hamburg, Germany, DESY (1992);
K.C. Höger, *Proc. Workshop on Physics at HERA*, W. Buchmüller and G. Ingelman (eds.), Vol. 1, p. 43. Hamburg, Germany, DESY (1992).

[24] L3 Collaboration, M. Acciarri et al., Phys. Lett. B 502 (2001) 37.

[25] DELPHI Collaboration, P. Abreu et al., Eur. Phys. J. C 8 (1999) 41.

Decay Mode	Background processes	Data	Predicted background
$e^* \to e\gamma$	NC, QED-Compton	18	20.1 ± 1.2
$e^* \to \nu W \to \nu q'\bar{q}$	CC DIS, PHP	13	13.9 ± 1.1
$e^* \to eZ \to eq\bar{q}$	NC DIS	32	32.9 ± 1.1
$e^* \to eZ \to e\nu\bar{\nu}$	NC DIS, W, CC DIS	1	4.1 ± 0.6
$q^* \to q\gamma$	Prompt γ, PHP, NC DIS	11	19.0 ± 1.9
$q^* \to qW \to qe\nu$	NC DIS, W, CC DIS	4	4.1 ± 0.6
$\nu^* \to \nu\gamma$	CC DIS	2	1.5 ± 0.2
$\nu^* \to \nu Z \to \nu q\bar{q}$	CC DIS, PHP	16	13.5 ± 0.6
$\nu^* \to eW \to eq'\bar{q}$	NC DIS	20	15.0 ± 1.3

Table 1: *The excited-fermion decay modes, main backgrounds and numbers of events that pass the selection criteria for the different channels compared with the Monte Carlo background predictions. The abbreviations of the background processes are defined in the text. The e^* and q^* results are from $47.7\,pb^{-1}$ of e^+p data and the ν^* results are from $16.7\,pb^{-1}$ of e^-p data. The uncertainties on the background predictions are statistical only.*

Decay Mode	Resolution (GeV)		Efficiency (%)	
	125 GeV	250 GeV	125 GeV	250 GeV
$e^* \to e\gamma$	1.0	2.2	66	78
$e^* \to \nu W \to \nu q'\bar{q}$	5.1	9.5	48	50
$e^* \to eZ \to eq\bar{q}$	3.3	6.0	27	52
$e^* \to eZ \to e\nu\bar{\nu}$	3.3	8.2	58	82
$q^* \to q\gamma$	4.7	9.1	55	67
$q^* \to qW \to qe\nu$	7.6	19.0	46	38
$\nu^* \to \nu\gamma$	5.6	5.3	55	61
$\nu^* \to \nu Z \to \nu q\bar{q}$	8.3	17.2	39	66
$\nu^* \to eW \to eq'\bar{q}$	14.4	15.3	49	51

Table 2: *Gaussian mass resolutions and selection efficiencies for excited fermions with masses of 125 and $250\,GeV$.*
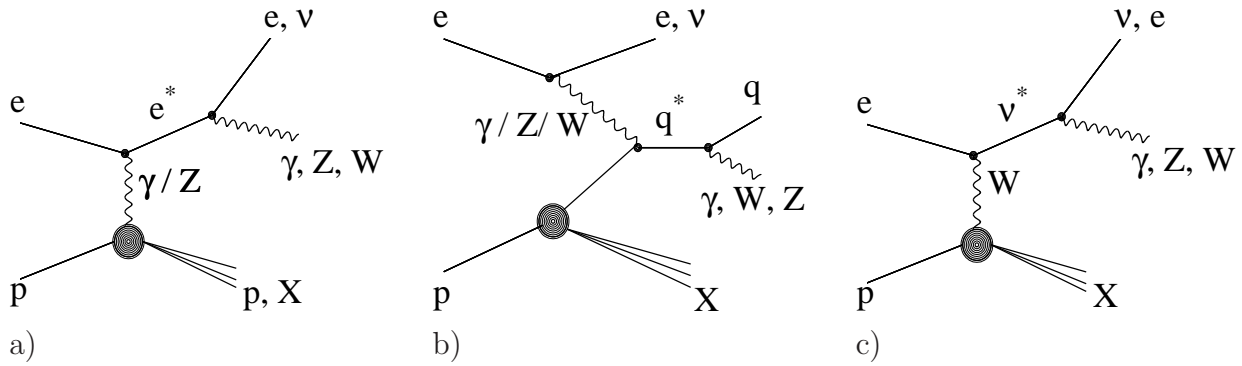
Figure 1: *Diagrams considered for the production of (a) excited electrons, (b) excited quarks and (c) excited neutrinos in ep collisions, with their decays into a known fermion and a gauge boson.*
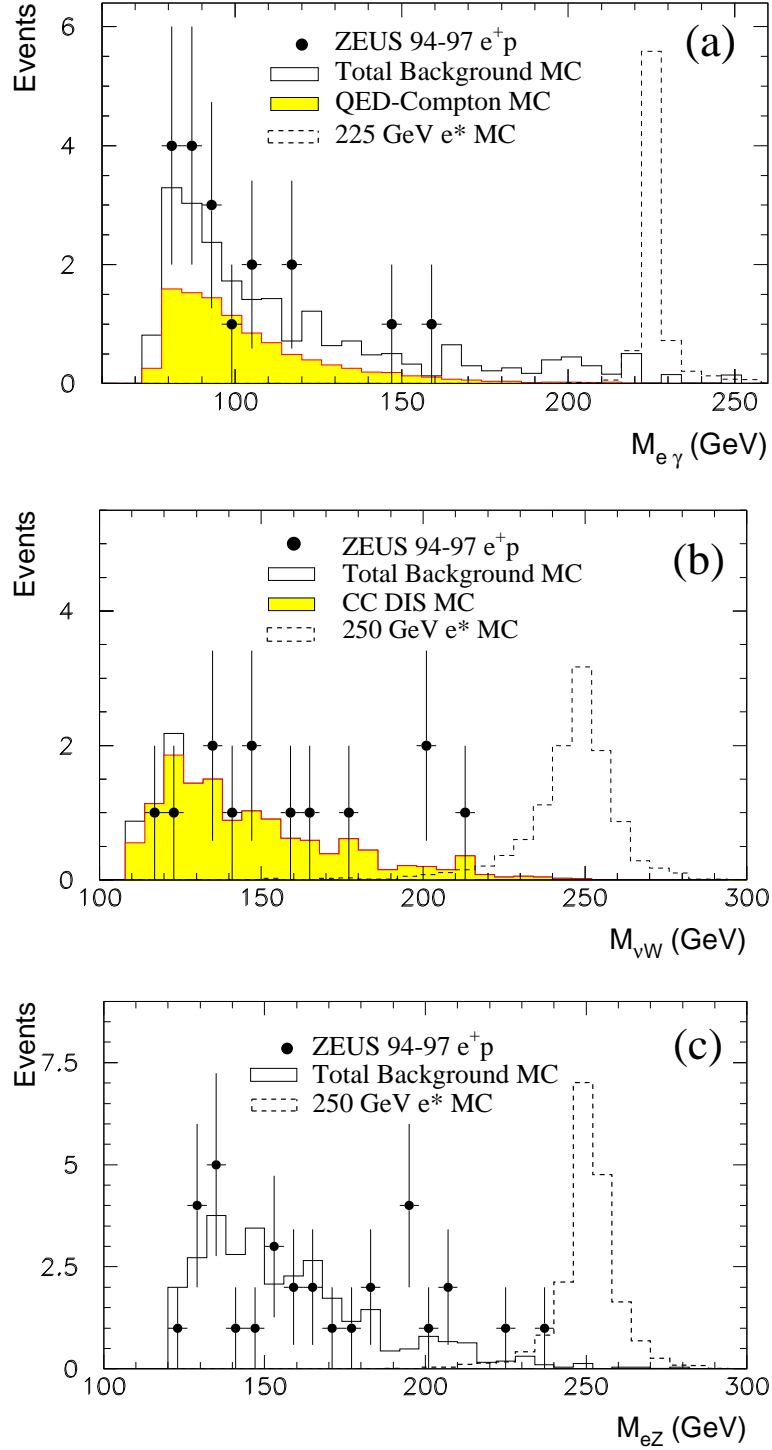
ZEUS

Figure 2: *Invariant-mass distributions for (a) $e^* \to e\gamma$, (b) $e^* \to \nu W \to \nu q'\bar{q}$ and (c) $e^* \to eZ \to eq\bar{q}$. Examples of e^* signals are shown as the dashed histograms (arbitrary normalisation) to illustrate the mass resolution.*
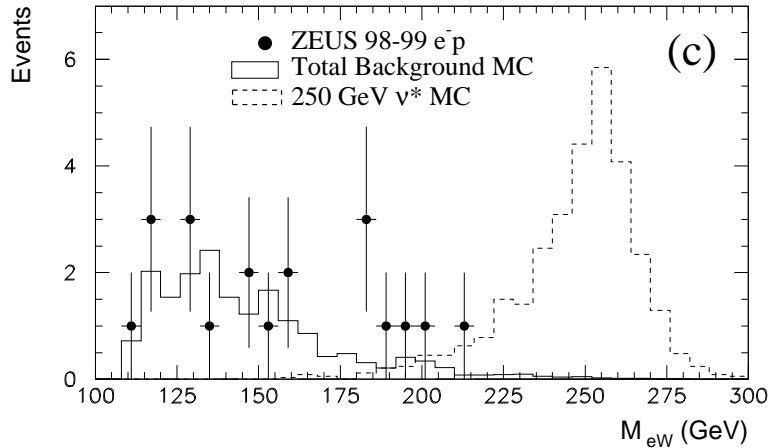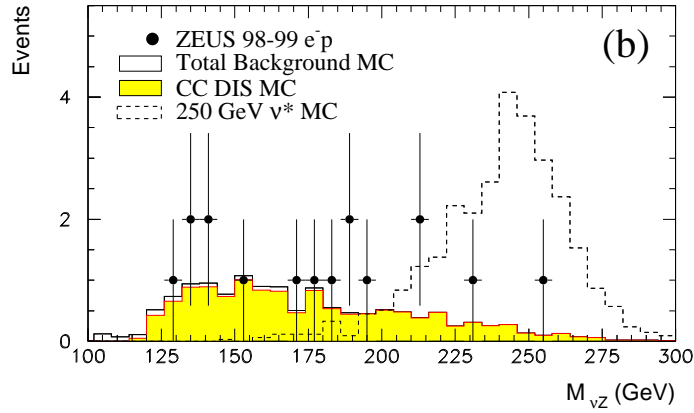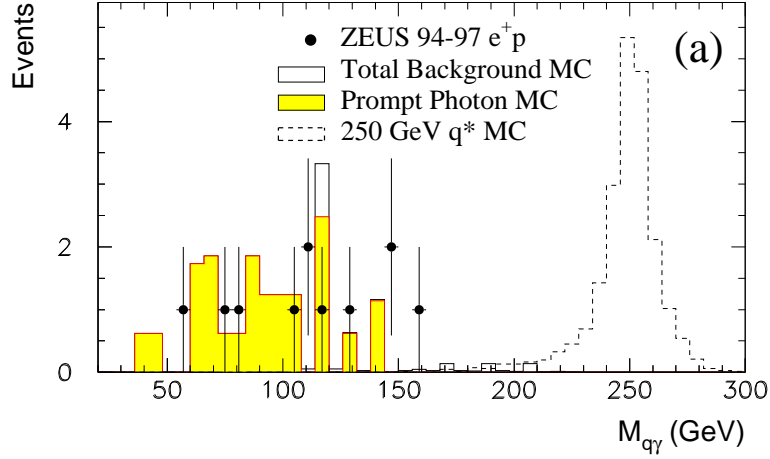
15

ZEUS

Figure 3: *Invariant-mass distributions for (a) $q^* \to q\gamma$, (b) $\nu^* \to \nu Z \to \nu q\bar{q}$ and (c) $\nu^* \to eW \to eq'\bar{q}$. Examples of q^* and ν^* signals are shown as the dashed histograms (arbitrary normalisation) to illustrate the mass resolution.*
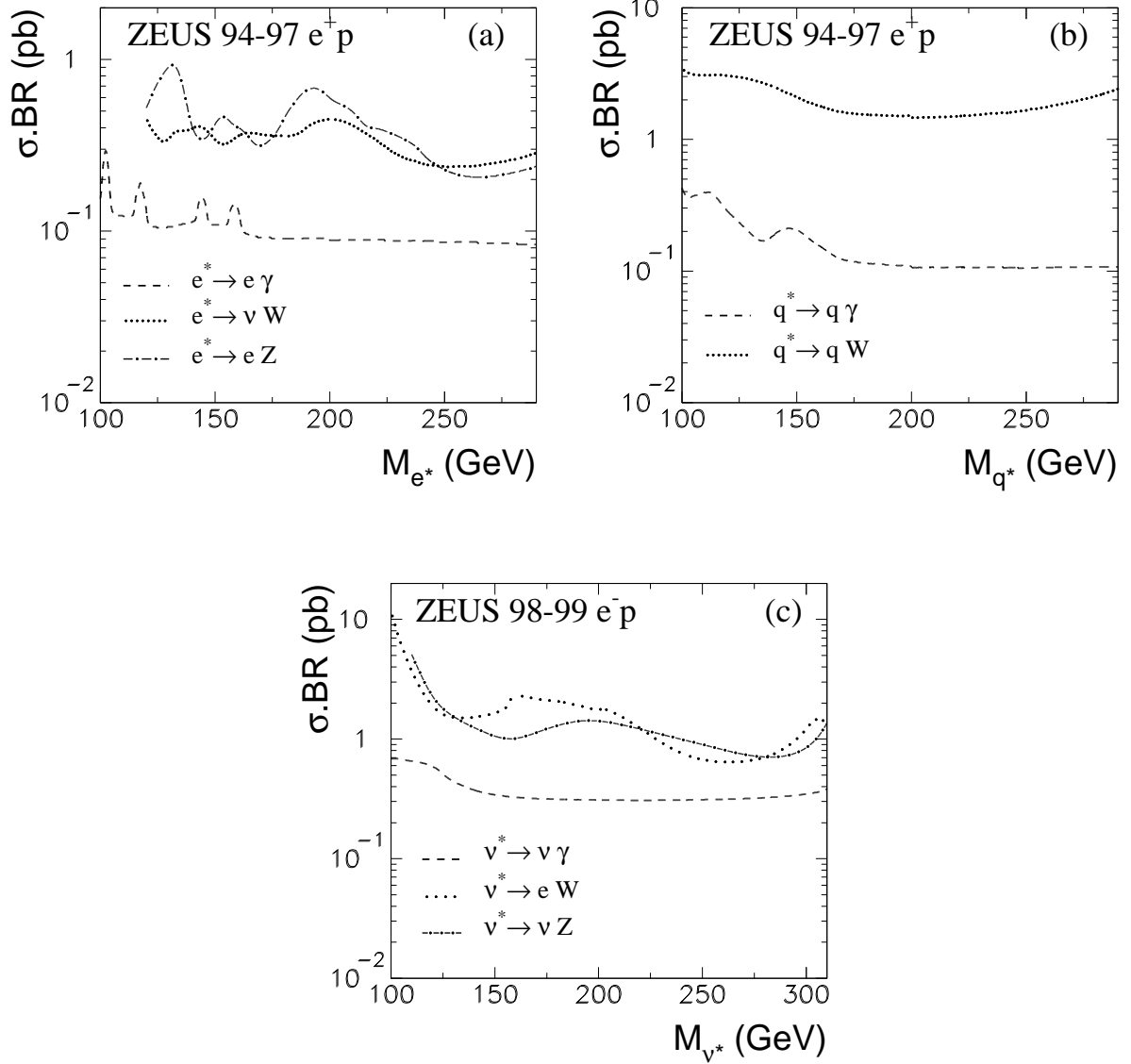
ZEUS

Figure 4: *Upper limits at 95% confidence level on the production cross section times the branching ratio as a function of the excited-fermion mass for (a) $e^* \to e\gamma$, $e^* \to \nu W$, $e^* \to eZ$, (b) $q^* \to q\gamma$, $q^* \to qW$ and (c) $\nu^* \to \nu\gamma$, $\nu^* \to eW$, $\nu^* \to \nu Z$. In all cases, the areas above the lines are excluded.*
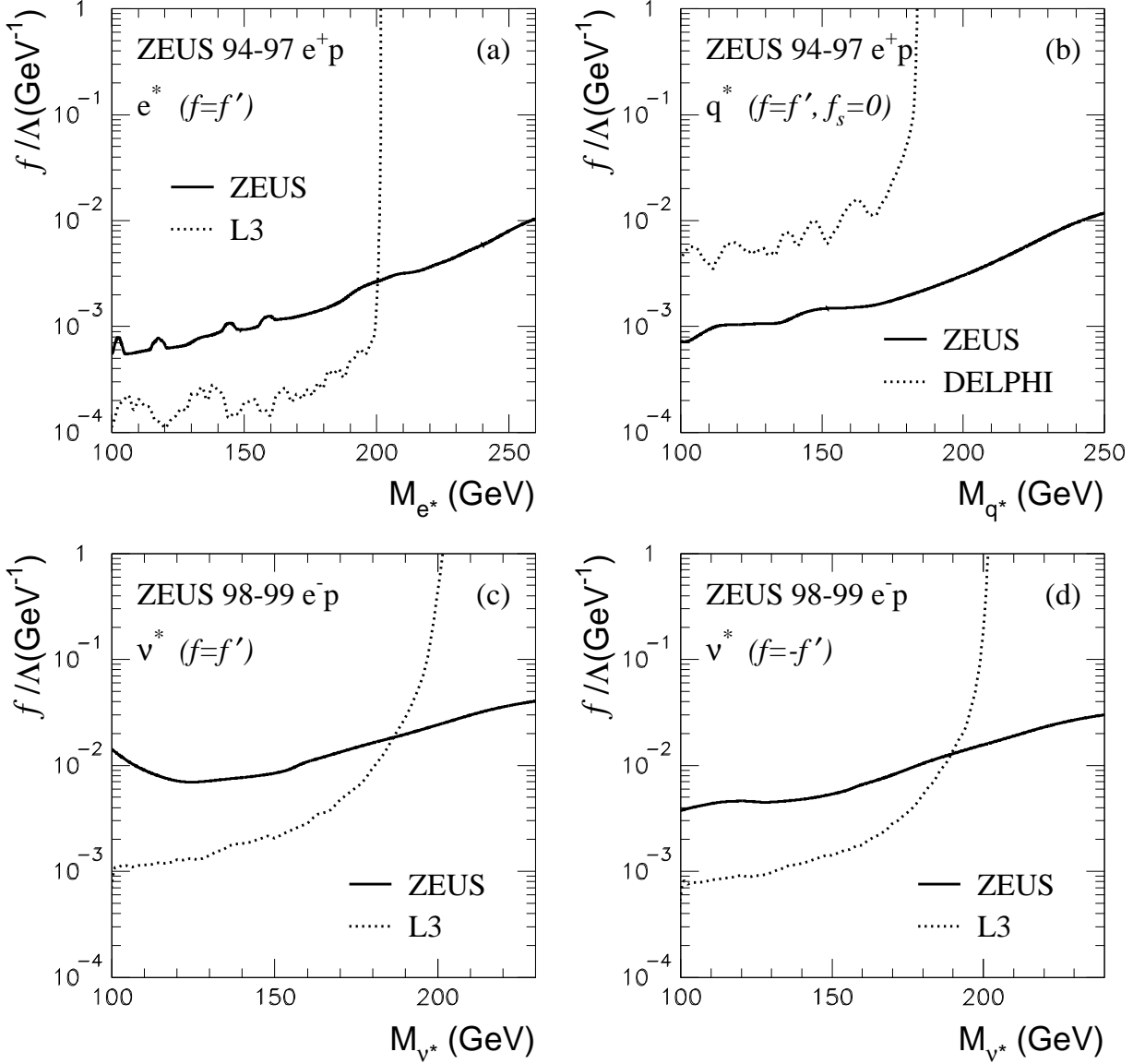
ZEUS

Figure 5: *Upper limits at 95% confidence level on the coupling f/Λ as a function of the excited-fermion mass for (a) excited electrons assuming $f = f'$, (b) excited quarks assuming $f = f'$, $f_s = 0$, (c) excited neutrinos assuming $f = f'$ and (d) excited neutrinos assuming $f = -f'$. The solid curves result from combining all channels. The dotted lines are the limits from L3 [24] and DELPHI [25]. The DELPHI limit on q^* was derived assuming $BR(q^* \to q\gamma) = 1$. In all cases, the areas above the lines are excluded.*